An inhibitor of tau hyperphosphorylation prevents severe motor impairments in tau transgenic mice

Sylvie Le Corre*†, Hans W. Klafki*‡, Nikolaus Plesnila§, Gabriele Hübinger*, Axel Obermeier*, Heidi Sahagún*, Barbara Monse*, Pierfausto Seneci*¶, Jada Lewis‖, Jason Eriksen‖, Cynthia Zehr‖, Mei Yue‖, Eileen McGowan‖, Dennis W. Dickson‖, Michael Hutton‖**, and Hanno M. Roder*††

*Sirenade Pharmaceuticals, Am Klopferspitz 19a, 82152 Martinsried, Germany; §Experimental Neurosurgery Institute for Surgical Research, Ludwig–Maximilian University Munich, Marchioninistrasse 15, 81377 Munich, Germany; and ‖Department of Neuroscience, Mayo Clinic, 4500 San Pablo Road, Birdsall Building 210, Jacksonville, FL 32224

Communicated by Vernon Martin Ingram, Massachusetts Institute of Technology, Cambridge, MA, April 14, 2006 (received for review September 22, 2005)

An orally bioavailable and blood–brain barrier penetrating analog of the kinase inhibitor K252a was able to prevent the typical motor deficits in the tau (P301L) transgenic mouse model (JNPL3) and markedly reduce soluble aggregated hyperphosphorylated tau. However, neurofibrillary tangle counts were not reduced in the successfully treated cohort, suggesting that the main cytotoxic effects of tau are not exerted by neurofibrillary tangles but by lower molecular mass aggregates of tau. Our findings strongly suggest that abnormal tau hyperphosphorylation plays a critical role in the development of tauopathy and suggest a previously undescribed treatment strategy for neurodegenerative diseases involving tau pathology.

Alzheimer's disease | extracellular signal-regulated kinase inhibitor | paired helical filament | tangles

Neurofibrillary lesions composed of hyperphosphorylated and aggregated forms of the microtubule-associated protein tau represent characteristic hallmarks of several neurodegenerative disorders including Alzheimer's disease (AD), frontotemporal dementia with parkinsonism linked to chromosome 17 (FTDP-17), and others (reviewed in ref. 1). Compelling evidence that tau malfunction or dysregulation alone can be sufficient to cause neurodegeneration comes from the identification of mutations in the tau gene that cause FTDP-17 (2, 3).

Abnormal hyperphosphorylation of the tau protein appears to be an early and pivotal event in the pathogenesis of AD and other tauopathies (4). Hyperphosphorylation interferes with the normal function of tau by abrogating the ability of tau to stabilize and promote the assembly of microtubules (5). Phosphorylation is sufficient to induce this loss of function as dephosphorylation of pathological tau proteins by phosphatases restores the microtubule-stabilizing activity of tau *in vitro* (6). These observations suggest that abnormal hyperphosphorylation of tau may play a role in the pathogenesis of tauopathies by inducing microtubule network breakdown, followed by neuritic atrophy and neurodegeneration. Additionally, hyperphosphorylated and/or aggregated species of tau may exert direct toxic effects on neurons (7). It is important to recognize, however, that most phosphorylation-related antigenic markers of tau also are found in the normal brain, if postmortem dephosphorylation artifacts are minimized and can be reconstituted *in vitro* by a broad range of proline-directed kinases (8). Indeed, basal phosphorylation levels at some of these sites within tau are thought to play an important role in the normal regulation of tau function and microtubule dynamics (9).

Although it is clear that aberrant phosphorylation of the tau protein is a defining and invariable feature of the neurofibrillary tangles (NFTs) and neuropil threads (NTs) in AD, the multitude of phosphorylation sites within tau and the complexity of the resulting phosphorylation patterns has hindered the unambiguous identification of the relevant protein kinases contributing to both normal and abnormal phosphorylation under pathological conditions. Various kinases have been implicated specifically in abnormal hyperphosphorylation of the 17 Ser/Thr-Pro motifs mainly responsible for the diagnostic antigenic properties of pathological tau species (reviewed in refs. 8 and 10). extracellular signal-regulated kinase (ERK) 2 has been a particularly conspicuous candidate because of its ability to phosphorylate all these sites up to the maximal stoichiometry (11, 12), an ability matched only by SAPK4 and to a slightly lesser degree by SAPK3 (ERK6) (13). Consequently even disease-specific tau phosphoepitopes, such as those related to certain Ser-422 phosphorylation-dependent epitopes (14), are fully reconstituted *in vitro* by ERK2, but not by other known tau-kinases like cdk5 or GSK3, which phosphorylate tau only to lower stoichiometric ratios. The finding that activated forms of ERK1 and ERK2 colocalize with the neurofibrillary lesions in postmortem AD brains (15, 16) also is compatible with a role for ERKs in the pathological hyperphosphorylation of tau.

Here we report a significant reduction in the levels of abnormal hyperphosphorylated tau species and prevention of the severe motor impairments in JNPL3 transgenic mice expressing P301L mutant human tau after chronic treatment with a previously undescribed small molecule inhibitor of ERK2, albeit one of limited selectivity. Our findings provide clear *in vivo* evidence that inhibition of pathological tau hyperphosphorylation can delay or prevent tau-related functional deficits and support the use of such inhibitors as an approach to developing a disease modifying treatment for tau-related neurodegenerative disease.

Results

Despite extensive screening efforts for small molecule inhibitors of ERK2, only the known natural product K252a produced useful inhibitory activity for ERK2, a hitherto unappreciated property of this otherwise well known compound (Fig. 1*B*). K252a was not specific for ERK2 but had comparable activity against cdk1 and moderate specificity (vs. PKC, PKA, and GSK3β) *in vitro* (G.H., S. Geis, S.L.C., S. Gordon, R. Francasso, S. Ferrand, H.W.K., and H.M.R., unpublished data). A medicinal chemistry program therefore was initiated to optimize the K252a lead structure for a proof of concept experiment in tau transgenic mouse models (17, 18).

NEUROSCIENCE

Conflict of interest statement: H.M.R. is a major shareholder of Tautatis, Inc., a company developing inhibitors of tau pathology.

Abbreviations: AD, Alzheimer's disease; ERK, extracellular signal-regulated kinase; NFT, neurofibrillary tangle; NT, neuropil thread.

†Present address: AMO Germany GmbH, Rudolf-Plank-Strasse 31, 76275 Ettlingen, Germany.

‡Present address: Department of Psychiatry and Psychotherapy, University of Erlangen-Nuremberg, Schwabachanlage 6, 91052 Erlangen, Germany.

¶Present address: Department of Organic and Industrial Chemistry, University of Milan, Via Venzian 21, 20100 Milan, Italy.

**To whom correspondence should be addressed. E-mail: hutton.michael@mayo.edu.

††Present address: Tautatis, Inc., 124 Mount Auburn Street, Suite 200N, Cambridge, MA 02138.

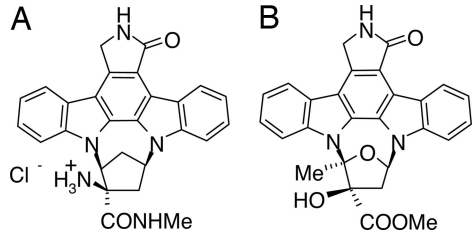

Fig. 1. Chemical structure and pharmacokinetics of SRN-003-556. (*A* and *B*) SRN-003-556 (*A*) is an orally bioavailable CNS-penetrating synthetic analog of K252a (*B*).

In keeping with the unusually restrictive inhibitor-binding site of ERK2, apparent from the initial round of compound screening, major structural alterations to the K252a scaffold did not yield improved inhibitory activity. However, of all of the K252a derivatives tested, those that inhibited ERK2 consistently blocked tau hyperphosphorylation induced by okadaic acid in cell and brain slice culture models (H. Roder, unpublished observations). SRN-003-556 (Fig. 1*A*) is a synthetic indolocarbazole analogue of K252a (Fig. 1*B*), which was substantially superior to K252a and other analogs with respect to oral bioavailability and brain penetration. However, the moderate selectivity of K252a (ERK2 = cdk1 > PKA, GSK3, PKC) (G.H., S. Geis, S.L.C., S. Gordon, R. Fracasso, S. Ferrand, H.W.K., and H.M.R., unpublished data) was essentially lost with SRN-003-556. The compound inhibited ERK2, cdc2, GSK3-β, PKA. and PKC *in vitro* in the presence of 250 μM of ATP with IC_{50} values of 0.6, 0.18, 0.35, 0.44, and 0.26 μM, respectively.

Pathological hyperphosphorylation of tau at multiple proline directed serine and threonine sites, as induced by okadaic acid, was potently prevented by SRN-003-556 in adult rat hippocampal slices (Fig. 2). Remarkably SRN-003-556 treatment (Fig. 2) resulted in inhibition of tau phosphorylation at the promiscuous AT8 phosphoepitope (site related to pS202/T205) and the pathospecific AP422 phosphoepitope (site related to pS422) (mean IC_{50} ± SD: AT8, 0.6 ± 0.19 μM; AP422, 0.8 ± 0.18 μM). Additionally, the IC_{50} for a phosphoepitope related to the nonproline-directed Ser-262 site in the microtubule-binding domain and not subject to direct ERK2 phosphorylation was nearly coincident (anti-pS262: 0.5 ± 0.22 μM). Despite the low kinase specificity *in vitro*, 1 μM SRN-003-556 did not induce metabolic toxicity in SHSY5Y cells based on analysis of intracellular ATP concentrations, whereas an *in vitro* cell viability assay with primary human hepatocytes indicated cytotoxicity with an EC_{50} of 22 μM.

To adjust the oral dosing of the compound to match the target concentration in brain as determined by the brain slice model critical pharmacokinetic parameters relating to half-life in plasma and C_{max} in plasma and brain were determined in C57BL/6NCrl mice (Charles River Laboratories). Maximal concentrations of 1.8 μM in the brain, 5 μM in the spinal cord, and 3 μM in the plasma (n = 3) were detected 1 h after oral dosing of 30 mg/kg SRN-003-556 in food-deprived mice. Compound levels declined at 3 h after dosing to 0.7 μM in the brain, 1.5 μM in the spinal cord, and 1.4 μM in the plasma. Compound levels in all tissues dropped to <0.5 μM after 6–8 h. Oral bioavailability (26%) and good brain penetration were corroborated in rats where plasma C_{max} (after 4 h) and $t_{1/2}$ after oral gavage at a dose of 15 mg/kg were 1.65 μM and 2.6 h, respectively (n = 3), with a nearly equal concentration in brain (data not shown).

To examine the ability of SRN-003-556 to inhibit the progression of tauopathy *in vivo*, we used the well characterized JNPL3 transgenic mice expressing mutant human P301L 4R0N tau. Expression of this FTDP-17-linked mutant form of tau in these mice results in age-dependent development of NFTs, neuronal loss, and progressive motor deficits (19). Importantly, the major hyperphosphorylated detergent-insoluble tau species, which accumulates in this model, comigrates at an apparent molecular mass of 64 kDa with hyperphosphorylated forms of the 4R0N splice-isoform in detergent-insoluble tau preparations from human AD brains (so called "PHF" tau) on SDS/PAGE, and displays the typical phosphoepitope profile of PHF-tau (20). These observations suggest that the biochemical mechanism of tau hyperphosphorylation in AD is recapitulated in an authentic way in the JNPL3 mice.

For the dosing study, 72 hemizygous female transgenic JNPL3 mice were divided into two matched groups. Treatment with SRN-003-556 or vehicle (PEG 400) started at 229 days of age, when one mouse from each cohort showed initial signs of motor deficits (these two pilot animals were excluded from the data analysis). The study design was based on the remaining 70 JNPL3 mice from the

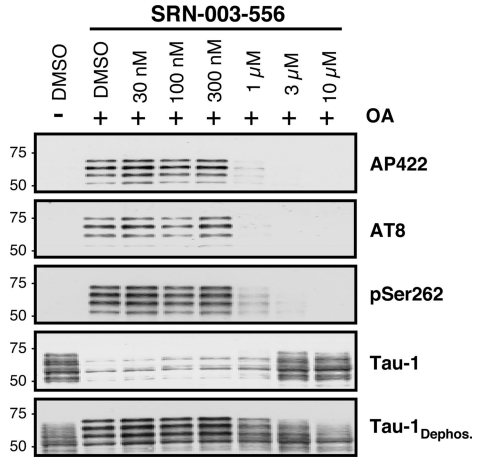

Fig. 2. SRN-003-556 prevents okadaic acid-induced tau hyperphosphorylation in rat hippocampal slices in a dose-dependent manner. Four hundred fifty-micrometer slices were prepared from hippocampi of adult Wistar rats in artificial cerebrospinal fluid buffer. SRN-003-556 was added 90 min before addition of okadaic acid (1 μM final concentration). After another 90 min, the slices were extracted and analyzed by Western blotting with phosphospecific antibodies: AP422, AT8, anti-pSer262, and Tau-1, which detects tau protein when unphosphorylated at residues 189–207. For normalization to total tau, blotted proteins were dephosphorylated exhaustively on the blot with excess alkaline phosphatase and reprobed with Tau-1.

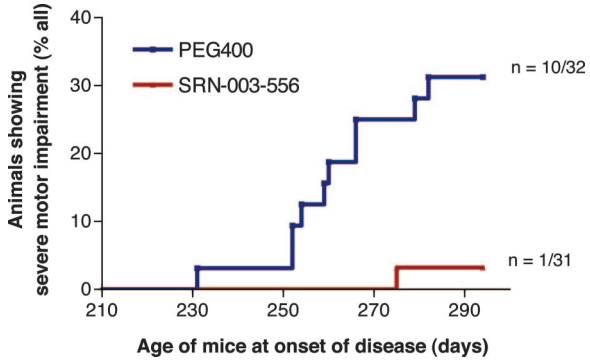

Fig. 3. SRN-003-556 delays/prevents the onset of motor deficits in JNPL3 mice. Starting at age 229 days, hemizygous P301L-tau transgenic female JNPL3Hlmc mice were treated twice daily with alternating doses of SRN-003-556 by oral gavage for 9 weeks. Control animals received the PEG 400 vehicle alone. Mice were food deprived 4 h before application. Mice received 100 μl of SRN-003-556 (3.2 mg/ml in PEG 400; 10 mg/kg) at 1000 hours and another 200 μl (20 mg/kg) at 1600 hours. Motor performance was tested in regular intervals with a set of formal staging criteria. The survival curve shows the number of animals that reached severe phenotypic stage in the equally sized control group and the treated group. The difference between the two groups was highly significant (P = 0.0033; log-rank test).

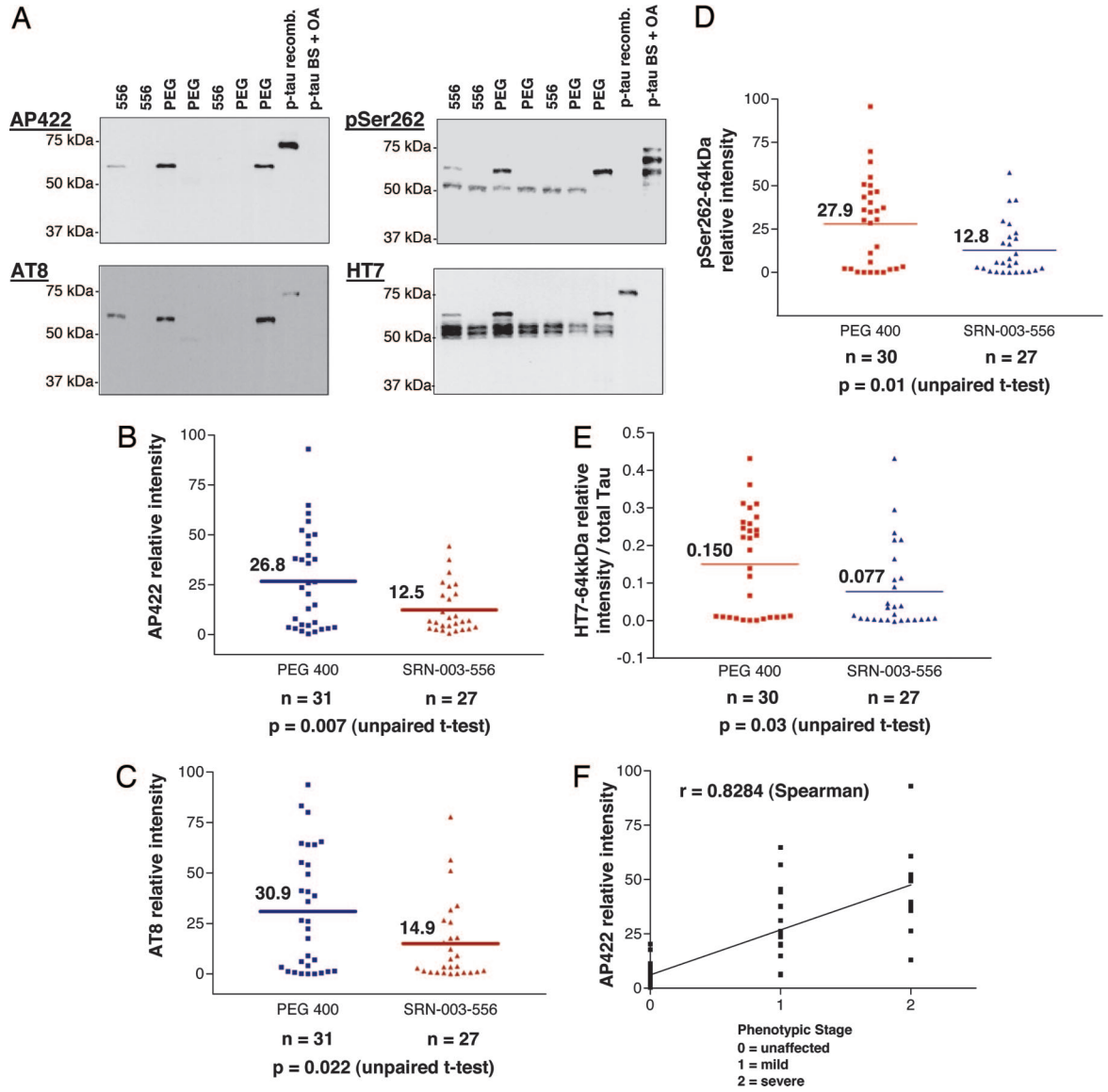

Fig. 4. JNPL3Hlmc transgenic mice treated with SRN-003-556 have reduced levels of soluble aggregated 64-kDa hyperphosphorylated tau species. Tau proteins were extracted from spinal cord tissue and analyzed by Western blotting with phosphospecific antibodies AP422, AT8, and anti-pS262, followed by normalization of the signals for exposure and expression/loading. (*A*) AP422 and AT8 antibodies detected only the 64-kDa tau species, whereas anti-pS262 also detected the normal tau species (≈55 kDa). Quantification of the blots revealed significantly lower levels of the pathological 64-kDa tau species in the treated group compared with the vehicle group by the criteria of normalized immunoreactivities with AP422 (*B*), AT8 (*C*), anti-pS262 (*D*), and HT7 (*E*). (*F*) Representative for all 64-kDa tau markers, AP422 signals correlated well with phenotypic stage (Spearman *r*, 0.8284; $P < 0.0001$).

compound and vehicle-treated cohorts ($n = 35$) developing "severe" motor deficits as a phenotypic endpoint. "Severe" motor impairment was defined by a dual set of tests, i.e., a wire hang test and a beam balance test (see *Materials and Methods* for experimental details). Composite failure criteria were chosen that were sufficiently stringent to exclude false positives (i.e., mice that recover after incidental performance slips). Under these criteria, during a 9-week treatment period, with a twice daily oral dosing regimen of alternating 10 and 20 mg/kg doses, 10 of 32 mice from the vehicle-treated control group developed severe motor impairments with an onset of disease at 260.1 ± 14.6 days (mean ± SD). In contrast, only one of 31 mice treated with SRN-003-556 reached this severe phenotypic stage at the age of 275 days, indicating that SRN-003-556 significantly delayed or prevented the development of motor deficits ($P = 0.0033$ log-rank test) (Fig. 3). At the termination of the study, 12 mice from the control group and 20 from the treated group did not show any signs of motor impairments. Ten mice from each group were determined to have reached a mild or intermediate phenotypic stage after visual independent inspection by two investigators. Mild or intermediate stages were classified as motor deficits (e.g., abnormal gait or hind-limb scissoring) that did not reach the formal threshold used to define the severe stage (see *Materials and Methods* for experimental details). Blood and organs (liver, kidney, lung, stomach, and gut) of 20 animals across the phenotypic stages ($n = 10$ per group) were assessed for signs of toxicity, with special attention to potential cytotoxic or antiproliferative effects. No SRN-003-556-related signs of organ and tissue pathology and no abnormal clinical chemistry parameters, including pH, ions, hematocrit, and blood cell counts (RBC, WBC, neutrophils, and platelets) were observed after chronic 9-week exposure.

To gain insights into the mechanism of the prevention or delay of the phenotype in the SRN-003-556-treated mice, we performed neuropathological and biochemical analyses on brain and spinal

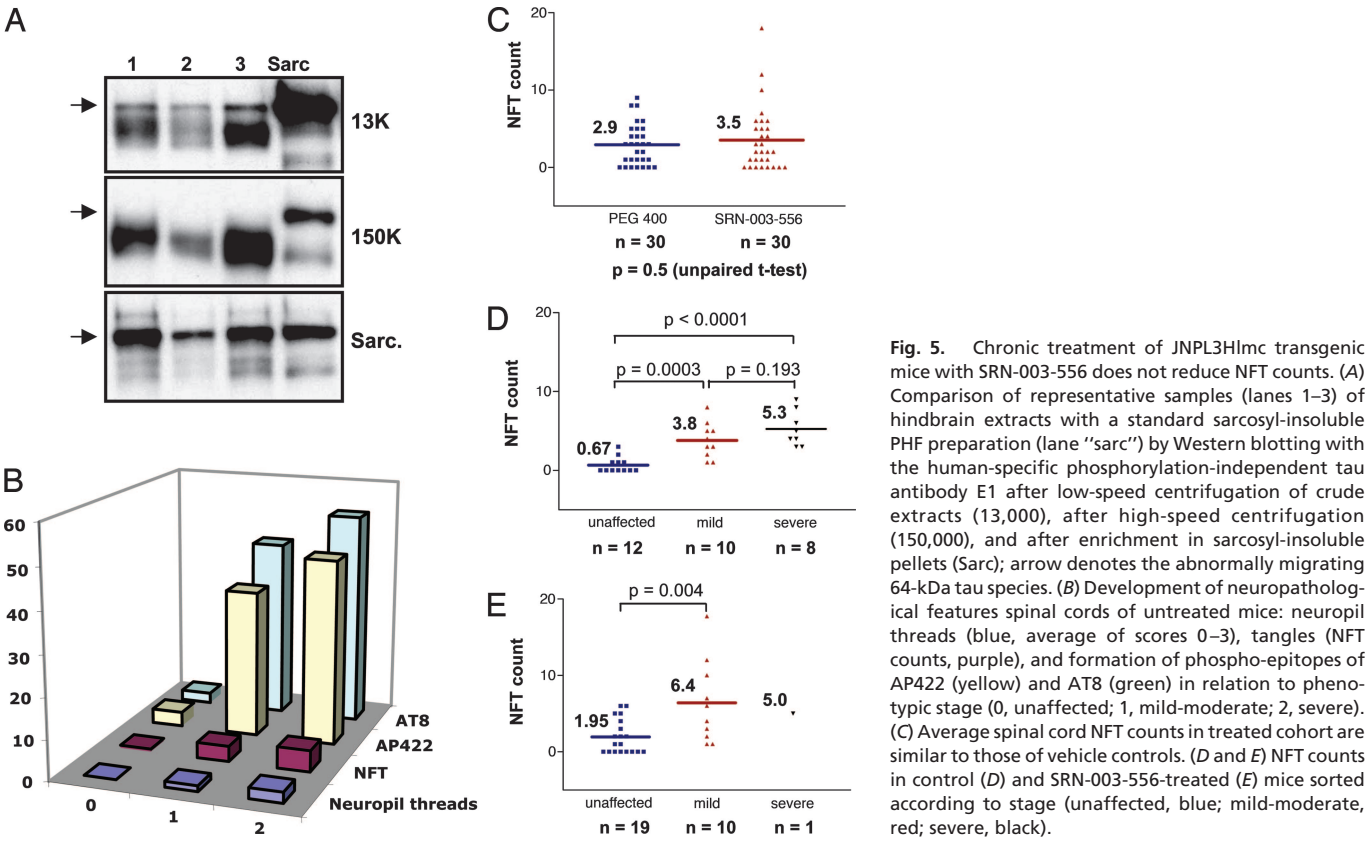

Fig. 5. Chronic treatment of JNPL3Hlmc transgenic mice with SRN-003-556 does not reduce NFT counts. (*A*) Comparison of representative samples (lanes 1–3) of hindbrain extracts with a standard sarcosyl-insoluble PHF preparation (lane ''sarc'') by Western blotting with the human-specific phosphorylation-independent tau antibody E1 after low-speed centrifugation of crude extracts (13,000), after high-speed centrifugation (150,000), and after enrichment in sarcosyl-insoluble pellets (Sarc); arrow denotes the abnormally migrating 64-kDa tau species. (*B*) Development of neuropathological features spinal cords of untreated mice: neuropil threads (blue, average of scores 0–3), tangles (NFT counts, purple), and formation of phospho-epitopes of AP422 (yellow) and AT8 (green) in relation to phenotypic stage (0, unaffected; 1, mild-moderate; 2, severe). (*C*) Average spinal cord NFT counts in treated cohort are similar to those of vehicle controls. (*D* and *E*) NFT counts in control (*D*) and SRN-003-556-treated (*E*) mice sorted according to stage (unaffected, blue; mild-moderate, red; severe, black).

cord tissue from SRN-003-556-treated and control mice. To examine the phosphorylation state of tau proteins, spinal cord tissue was homogenized in detergent-free kinase/phosphatase inhibitory buffers followed by a low-speed centrifugation (13,000 × *g*). The supernatants then were subjected to Western blot analysis by using a phosphorylation state-independent antibody (HT7) specific for human tau and three phosphoepitope antibodies: AP422, AT8, anti-pS262, and anti-pThr231 that recognize epitopes related to pS422, pS202/T205, pS262, and pT231, respectively. Western blot analysis (Fig. 4*A*) of human tau in the low-speed supernatants, with HT7, demonstrated the clear resolution of the pathologically hyperphosphorylated human tau band (64-kDa species) from the mixture of normal human tau proteins (55- to 60-kDa species) by virtue of its greatly retarded gel mobility. Signals of all tau-related bands were quantified by densitometry and corrected for exposure variation by reference to an appropriate phospho-tau standard on each blot (see Fig. 4). Signals of the 64-kDa tau species were normalized further to total human tau levels (55–60 kDa plus 64 kDa), as determined with the HT7 antibody, to correct for variation in transgenic tau expression levels. Both phosphoepitope-specific antibodies AP422 and AT8 detected only a single hyperphosphorylated tau species corresponding to the pathological 64-kDa tau species. Importantly, the 64-kDa tau signals in spinal cord showed a strong correlation with the phenotypic stage of the mice (Fig. 4*F*). Levels of the 64-kDa pathological phospho-tau species were significantly lower in the SRN-003-556-treated animals compared with control mice (AP422: 53% reduction; $P = 0.0072$; AT8: 52% reduction; $P = 0.0215$; Fig. 4 *B* and *C*), although the average amounts of total expressed human tau (55–60 kDa plus 64 kDa) were not significantly different between the two groups (total HT7 signal, treated group: 88% of control; $P = 0.639$). A similar link between the amount of the 64-kDa tau species and levels of phospho-tau detected by the anti-pT231 antibody also was noted (data not shown). The anti-pS262 pAb and the HT7 mAb detected not only the 64-kDa hyperphosphorylated tau species but also normal tau proteins in the basal phosphorylation state between 55 and 60 kDa (Fig. 4*A*). The normalized 64-kDa tau signal with both HT7 and anti-pSer262 also was reduced in the treated group to approximately half the intensity found in the control cohort (anti-pSer262: 54% reduction, $P = 0.0096$; Fig. 4*D*; HT7: 49% reduction, $P = 0.0321$; Fig. 4*E*) similar to the AT8 and AP422 proline-directed phosphoepitopes (Fig. 4 *D* and *E*). However, the phosphorylation state at Ser-262 of the normal tau proteins (55–60 kDa) was not significantly different in the treatment (SRN-003-556) group vs. controls (anti-pS262: 116% of control; $P = 0.8$).

Formation of the 64-kDa pathological tau species also was reduced to a lesser and not quite significant degree in low speed (13,000 × *g*) supernatants from hindbrain samples from the mice (AT8: 26.5%; $P = 0.08$) and similarly in 64-kDa tau-enriched sarkosyl-insoluble preparations from hindbrain (25.3%; $P = 0.125$). The smaller reduction in 64-kDa tau in the hindbrain compared with the spinal cord may reflect a dose–response type relationship by virtue of the lower levels of SRN-003-556 in brain vs. spinal cord (based on the pharmacokinetic data for SRN-003-556 in brain vs. spinal cord described above). Importantly, the pathological 64-kDa tau species almost was completely removed from the low speed (13,000 × *g*) supernatant fraction by centrifugation at 150,000 × *g* (Fig. 5*A*). This finding demonstrates that this hyperphosphorylated low-speed supernatant species constitutes mainly aggregated tau.

To examine the effects of SRN-003-556 on neuropathological changes in the brains of JNPL3 mice, we performed counts of NFTs and semiquantitative analysis of NTs in SRN-003-556-treated and vehicle-only mice. In the vehicle-treated cohort in this study, levels of low-speed soluble 64-kDa tau species and NFTs and NTs in the spinal cord increased in parallel with disease progression (Fig. 5*B*). The largest increases in NFTs, NTs, and 64-kDa tau all occurred with the phenotypic transition from the unaffected to the moderately affected state. Accordingly, in the control mice, spinal cord

NFT numbers correlated with disease stage ($r = 0.72$; Fig. 5*D*). Surprisingly, a clear break in the relationship between the histopathological and the biochemical markers becomes apparent in the comparison of spinal cord NFT counts in treated vs. vehicle-only JNPL3 mice where treatment with SRN-003-556 did not appear to reduce tangle numbers (Fig. 5*C* vs. Fig. 4 *B–E*) despite the observed reduction in the aggregated 64-kDa pathological tau species on Western blots described above. There was a nonsignificant trend toward higher NFT counts in the treated group as a whole (Fig. 5*C*) and, indeed, when sorted according to phenotypic stage, it became apparent that the unaffected and moderately affected mice treated with SRN-003-556 had a 2.9-fold and a 1.7-fold higher NFT count than the respective control groups, although this increase again did not reach significance (unaffected, $P = 0.071$; moderately affected, $P = 0.185$; Fig. 5 *D* and *E*). Consequently, the moderately affected mice in the SRN-003-556-treated group had NFT counts similar to those of severely diseased control mice. In contrast, the levels of the 64-kDa tau species, measured by Western blotting, were not significantly different between treated and control mice within phenotypically matched groups (data not shown) and correlated with phenotypic stage in both the treated and control mice.

Discussion

The data set of this study is consistent with the long suspected role of abnormal hyperphosphorylation in the formation and/or stabilization of aggregated pathological tau species (as assessed by direct biochemical criteria) and their role in the onset of functional deficits.

After 9 weeks of treatment with the kinase inhibitor SRN-003-556, we observed a significant delay or prevention of the typical motor impairments in JNPL3-transgenic mice and a concomitant selective reduction in pathological 64-kDa tau species, with its complement of pathological phosphoepitopes. This pathological 64-kDa form of tau represents a distinct low-speed soluble but high-speed sedimentable pool of aggregated tau. Given that transgenic mutant tau is the sole disease causing entity in this model, it is reasonable to assume that the prevention of the onset/progression of motor deficits is related causally to this inhibition of abnormal tau hyperphosphorylation. However, in view of the limited selectivity of the SRN-003-556 kinase inhibitor, we cannot exclude that the therapeutic effects of the compound on the onset of motor deficits in JNPL3 mice are modified by unrelated pharmacological effects.

The observation that neither the average amounts of total expressed human tau (55–60 + 64 kDa) nor the phosphorylation state at Ser-262 of the normal tau proteins (55–60 kDa) were significantly different in the treatment (SRN-003-556) group vs. controls is evidence for a degree of specificity for the inhibition of tau hyperphosphorylation by SRN-003-556 *in vivo*, namely a differential effect of the kinase inhibitor, despite its limited selectivity, on the formation of the anti-pSer262 reactive pathological 64-kDa tau species, but there was no effect on the basal phosphorylation state at Ser-262 in normal tau proteins (55–60 kDa). This differentiation of abnormal from normal tau phosphorylation events *in vivo* is important in view of the likely role of phosphorylation in regulating the normal function of tau.

Based on numerous pathological studies, it is generally assumed that (*i*) abnormal hyperphosphorylation of tau is more or less directly related to its aggregation, (*ii*) the biochemically defined sarkosyl-insoluble pathological tau pool reflects the histopathologically defined NFTs and NTs, and (iii) the NFTs and NTs are direct correlates of synaptic deficits and neurodegeneration. However, the observations reported here indicate that the link between the formation of such biochemically defined abnormal tau species and histologically defined NFTs may be less direct than previously assumed. The functional benefits we observed in JNPL3 mice after 9 weeks treatment with SRN-003-556 track with the reduction in low-speed soluble hyperphosphorylated tau levels but not with NFT counts, which apparently continued to develop despite partial inhibition of pathological tau hyperphosphorylation. It appears likely that the roughly 50% inhibition of the formation of the hyperphosphorylated 64-kDa tau species is sufficient to reduce/prevent the neuronal dysfunction and neurodegeneration that underlies the onset of the motor phenotype in JNPL3 mice but is insufficient to retard the formation of NFTs or to reduce the number of neurons developing tangles. This scenario could reflect the amyloid-like nature of tau filaments that likely require lower levels of pathological tau proteins to drive continued aggregation after initial nucleation; however, we also cannot exclude the possibility that less pathological tau is incorporated into the same number of developing NFTs in SRN-003-556-treated mice.

The results in the JNPL3 mice treated with SRN-003-556 are consistent with the continued NFT formation observed in transgenic mice after suppression of 90% of mutant tau expression, despite remarkable functional improvement and inhibition of neuronal cell death (21). In addition, it has recently been observed in the Htau transgenic mouse model of tauopathy that neuronal cell death occurs independent of histologically observed tangles (22). These previous studies and our own data suggest that NFTs are not the main toxic entity in tauopathy, a situation reflected by recent insights in the area of Aβ peptide toxicity (23) and other CNS protein aggregation diseases, like CJD and Huntington's disease (24, 25), where it is increasingly evident that the obvious histopathological lesions are not the major cause of neurodegeneration and the development of clinical symptoms. At this point, the relationship between the biochemical and histological features of tau pathology may be understood best in terms of different pools of hyperphosphorylated tau. The relatively nontoxic tangle pool seems to represent the stable default fate but has a limited rate or capacity of uptake. Excessively generated hyperphosphorylated tau accumulates in a lower molecular mass aggregated form and is likely the major neurotoxic entity. These pools may exist in a product/precursor relationship but also may constitute alternative fates of hyperphosphorylated tau species. The exact role of hyperphosphorylation in the formation of various tau polymers remains controversial, and our data does not directly address whether hyperphosphorylation is required for initial aggregation or is a secondary event perhaps involved in the stabilization of aggregated tau. In any case, the ability of the kinase inhibitor SRN-003-556 to delay or prevent the onset of severe motor deficits in JNPL3 mice, without obvious harmful side effects, would predict a favorable scenario for therapeutic intervention in human tauopathy with kinase inhibitors, even if of limited specificity.

Materials and Methods

Preparation and Treatment of Rat Hippocampal Slices. Four hundred fifty-micrometer hippocampal slices were prepared from 250- to 300-g male Wistar rats and preincubated for 20–30 min in oxygenated ice cold, artificial cerebrospinal fluid with low Ca^{2+} (26 mM $NaHCO_3$/3.5 mM KCl/1.5 mM KH_2PO_4/1.4 mM $MgSO_4$/0.01 mM $CaCl_2$/10 mM D-glucose), then for 35 min at 36°C, followed by another 35 min at 1.3 mM Ca^{2+}. SRN-003-556 was added at concentrations from 30 nM to 10 μM in 0.1% DMSO. After 90 min of preincubation, 1 μM okadaic acid was added for another 90 min. Slices were extracted with homogenization buffer (500 mM Hepes, pH 7.0/100 mM sodium pyrophosphate/2 mM EGTA/2 mM EDTA/2 mM sodium orthovanadate/1 mM DTT/1 μM okadaic acid/1× protease inhibitor mixture (Complete; Roche Diagnostics) by sonication (10–15 s) followed by centrifugation (13,000 × *g* at 4°C for 30 min).

SRN-003-556 Pharmacokinetics. Three to four female C57BL/6NCrl mice (Charles River Laboratory; 20–25 g) were randomly assigned per time point (0.5, 1, 3, 6, 8, and 24 h). Animals were deprived of food intake 4 hours before oral administration of SRN-003-556 of

NEUROSCIENCE

≈30 mg/kg in PEG 400. Mice were killed to recover plasma, brains, and spinal cords. SRN-003-556 was extracted from 100-μl samples of plasma mixed with 200 μl of concentrated ammonia solution and 200 μl of saturated NaCl solution. The mixture was extracted twice with 2 ml of ethylacetate (HPLC grade).

SRN-003-556 was extracted from CNS tissue by homogenization by sonication in 500 μl of saturated NaCl solution. After adding 200 μl concentrated of ammonia, extraction then was performed as with the plasma samples. Extraction efficiencies (usually 90–95%) were determined with plasma and CNS tissue homogenates spiked with known amounts of SRN-003-556. Quantitative analysis of the organic extracts was performed by HPLC with fluorescence detection at 284 nm (excitation) and 476 nm (emission) on a 5-μm RP 18 Select B 12.5 × 4.6 mm column (Merck) at a flow rate of 0.75 ml/min with isocratic elution at a temperature of 40°C with acetonitrile/water 60/40 (vol/vol).

Treatment of JNPL3 Mice with SRN-003-556. Seventy-two heterozygous female transgenic JNPL3Hlmc mice (Taconic Farms) were divided into two matching groups. Treatment with SRN-003-556 or vehicle (PEG 400) started at the age of 229 days. The compound was given by oral gavage twice a day to food-deprived mice at 10 mg/kg (100 μl of solution in PEG 400) and 20 mg/kg (200 μl of solution), respectively. During the course of the study, seven mice died without evidence of motor dysfunction ($n = 3$ in control group and $n = 4$ in treated group) and therefore were excluded from the study.

Motor function was monitored twice a week by wire hang, beam walk, and flight reflex tests and then once a day when the first signs of motor impairments became evident. Animals who showed at least two consecutive hang-test failures for two consecutive days and/or drops from the beam two consecutive times for two consecutive days and/or the animal failed once at the hang test and simultaneously falls once from the beam for two consecutive days were rated as having severe motor deficits and were killed. The remaining mice that appeared either unaffected throughout the whole study period or developed mild motor abnormalities below formal threshold criteria for removal were killed at the end of the study period at the age of 294 days. The statistical significance of the treatment effect between the groups was assessed by a one-way ANOVA Fisher's post hoc test.

Mice were deeply anesthetized with 150 mg/kg of a Ketamine/Xylazine mixture i.p. (Amersham Pharmacia, Upjohn, and Bayer), and brains were resected quickly after removal of the skullcap; spinal cord tissue as well as blood and other organs were collected thereafter. One brain hemisphere was fixed in 4% paraformaldehyde, and the other half was immediately homogenized by sonication in ice-cold homogenization buffer for Western blot analysis.

Western Blot Analysis of Brain Slice, Brain, and Spinal Cord Supernatants. The proximal part of resected spinal cords (≈2 cm) was fixed in 4% paraformaldehyde for neuropathological studies, whereas the remaining (distal) part and the hindbrains were subjected to Western blot analysis. CNS tissues were extracted with 300 μl of homogenization buffer per 50 mg tissue by ultrasonication followed by centrifugation (13,000 × *g* at 4°C for 15–30 min). Supernatants were adjusted to equal protein concentration, resolved by SDS/PAGE on precast 10% Tris/Glycine gels (Anamed, Darmstadt, Germany) and transferred to nitrocellulose membranes (Amersham Pharmacia Biotech), which were subsequently blocked for 1 h at room temperature with either 5% skim milk/3% BSA/TBST (1× TBS plus 0.05% Tween 20) or 3% BSA/TBST depending on the antibodies used. After incubation with primary antibodies under blocking conditions, proteins were detected with secondary antibody (peroxidase-linked anti-rabbit or anti-mouse IgG) and enhanced chemiluminescence (ECL; Amersham Pharmacia Biotech). For secondary probing of blots, previously bound antibodies were removed in stripping buffer (0.2 M glycine, pH 2.5/0.05% Tween) for 30 min at 60°C, and membranes were thoroughly washed in TBST. Tau immunoreactive bands were quantitated by digital densitometric scanning (Bio-Rad QUANTITY ONE imaging software). Tau phosphoepitope signals on separate blots were corrected for exposure by referencing to an appropriate phospho-tau standard on the same blot: recombinant htau40, exhaustively phosphorylated *in vitro* by a mixture of ERK2 and PKA, for AP422 (gift of M. Hasegawa, Tokyo Institute of Psychiatry, Tokyo) and AT8 (Innogenetics, Gent, Belgium); for anti-pSer262 (BioSource International, Camarillo, CA), an amount of 2 μg of total protein lysate of rat hippocampal slices treated with 1 μM okadaic acid (Sigma-Aldrich) as above. Signals were normalized further to total human tau expression and loading by probing stripped blots either with HT7 (Innogenetics) or with Tau-1 (Chemicon) after exhaustive dephosphorylation on the blot by incubation in 50 mM Tris·HCl, pH 8.5/0.1 mM EDTA/0.5 mM $MgCl_2$ containing 100 units/ml calf intestinal alkaline phosphatase (Promega) for 2 h at 37°C.

Extraction and Analysis of Sarkosyl-Insoluble Tau from Hindbrain. Sarkosyl insoluble tau was prepared as described in ref. 19 and analyzed by Western blotting as described above.

Neuropathological Analysis of Tau Lesions in Spinal Cord. Paraffin-embedded tissue sections of spinal cord were stained with the Gallyas silver impregnation method as modified by Braak *et al.* (26). The number of neurofibrillary tangles in three nonoverlapping microscopic fields from the anterior and intermediolateral gray matter was recorded. Fields were chosen to reflect the highest density of lesions. The density of argyrophilic neuropil threads was assessed semiquantitatively on a four-point scale: 0, none; 1, sparse; 2, moderate; 3, frequent.

1. Tolnay, M. & Probst, M. (1999) *Neuropathol. Appl. Neurobiol.* **25,** 171–187.
2. Hutton, M., Lendon, C. L., Rizzu, P., Baker, M., Froelich, S., Houlden, H., Pickering-Brown, S., Chakraverty, S., Isaacs, A., Grover, A., *et al.* (1998) *Nature* **393,** 702–705.
3. Spillantini, M. G., Murrell, J. R., Goedert, M., Farlow, M. R., Klug, A. & Ghetti, B. (1998) *Proc. Natl. Acad. Sci. USA* **95,** 7737–7741.
4. Braak, H. & Braak, E. (1995) *Neurobiol. Aging* **16,** 271–284.
5. Alonso, A. C., Zaidi, T., Grundke-Iqbal, I. & Iqbal, K. (1994) *Proc. Natl. Acad. Sci. USA* **91,** 5562–5566.
6. Wang, J. Z., Grundke-Iqbal, I. & Iqbal, K. (1996) *Mol. Brain Res.* **38,** 200–208.
7. Schahani, N. & Brandt, R. (2002) *Cell. Mol. Life Sci.* **59,** 1668–1680.
8. Johnson, G. V. & Hartigan, J. A. (1998) *Alzheimer's Dis. Rev.* **3,** 125–141.
9. Stoothoff, W. H. & Johnson, G. V. (2005) *Biochim. Biophys. Acta* **1739,** 280–297.
10. Buee, L., Bussiere, T., Buee-Scherrer, V., Delacourte, A. & Hof, P. R. (2000) *Brain Res. Rev.* **1,** 95–130.
11. Roder, H. M. & Ingram, V. M. (1991) *J. Neurosci.* **11,** 3325–3343.
12. Drewes, G., Lichtenberg-Kraag, B., Doring, F., Mandelkow, E. M., Biernat, J., Goris, J., Doree, M. & Mandelkow, E. (1992) *EMBO J.* **11,** 2131–2138.
13. Goedert, M., Hasegawa, M., Jakes, R., Lawler, S., Cuenda, A. & Cohen, P. (1997) *FEBS Lett.* **409,** 57–62.
14. Hasegawa, M., Jakes, R., Crowther, R. A., Lee, V. M., Ihara, Y. & Goedert, M. (1996) *FEBS Lett.* **384,** 25–30.
15. Perry, G., Roder, H., Nunomura, A., Takeda, A., Friedlich, A. L., Zhu, X., Raina, A. K., Holbrook, N., Siedlak, S. L., Harris, P. L. & Smith, M. A. (1999) *NeuroReport* **10,** 2411–2415.
16. Pei, J.-J., Braak, H., An, W. L., Winblad, B., Cowburn, R. F., Iqbal, K.& Grundke-Iqbal, I. (2002) *Brain Res. Mol. Brain Res.* **109,** 45–55.
17. Sahagun-Krause, H., Thillaye Du Boullay, O., Thillaye Du Boullay, V., Casiraghi, L., Klafki, H., Seneci, P., Braxmeier, T., Mueller, S., Froehner, W., Monse, B., *et al.* (2005) *Chem. Abstr.* **139,** 69413t.
18. Monse, B., Braxmeier, T., Ferrand, S., Gordon, S., Klafki, H., Lahu, G., Roder, H., Sahagun-Krause, H., Seneci, P. & Thillaye Du Boullay, O. (2004) *Chem. Abstr.* **141,** 38635d.
19. Lewis, J., McGowan, E., Rockwood, J., Melrose, H., Nacharaju, P., Van Slegtenhorst, M., Gwinn-Hardy, K., Paul Murphy, M., Baker, M., Yu, X., *et al.* (2000) *Nat. Genet.* **25,** 402–405.
20. Sahara, N., Lewis, J., DeTure, M., McGowan, E., Dickson, D. W., Hutton, M. & Yen, S. H. (2002) *J. Neurochem.* **83,** 1498–1508.
21. SantaCruz, K., Lewis, J., Spires, T., Paulson, J., Kotilinek, L., Ingelsson, M., Guimaraes, A., DeTure, M., Ramsden, M., McGowan, E., *et al.* (2005) *Science* **309,** 476–481.
22. Andorfer, C., Acker, C. M., Kress, Y., Hof, P. R., Duff, K. & Davies, P. (2005) *J. Neurosci.* **25,** 5446–5454.
23. Selkoe, D. J. (2004) *Nat. Cell Biol.* **6,** 1054–1061.
24. Mallucci, G., Dickinson, A., Linehan, J., Klohn, P. C., Brandner, S. & Collinge, J. (2003) *Science* **302,** 871–874.
25. Arrasate, M., Mitra, S., Schweitzer, E. S., Segal, M. R. & Finkbeiner, S. (2004) *Nature* **431,** 805–810.
26. Braak, H., Braak, E., Ohm, T. & Bohl, J. (1988) *J. Stain Technol.* **63,** 197–200.